Paneth cells mediated the response of intestinal stem cells at the early stage of intestinal inflammation in the chicken

Lingzi Yu,[1] Xiaochen Xie,[1] Keyang Jiang, Yi Hong, Zhou Zhou, Yuling Mi, Caiqiao Zhang, and Jian Li[2]

Department of Veterinary Medicine, Zhejiang Provincial Key Laboratory of Preventive Veterinary Medicine, College of Animal Sciences, Zhejiang University, Hangzhou 310058, P.R. China

ABSTRACT The rapid renewal and repair of the intestinal mucosa are based on intestinal stem cells (**ISC**), which are located at the crypt bottom. Paneth cells are an essential component in the crypt, which served as the niche for ISC development. However, in the chicken, how the function of Paneth cells changes during intestinal inflammation is unclear and is the key to understand the mechanism of mucosal repair. In the present study, 36 HyLine White chickens (7 d of age, n = 6) were randomly divided into 1 control and 5 lipopolysaccharide (**LPS**) injection groups. The chickens were injected (i.p.) with PBS in the control group, however, were injected (i.p.) with LPS (10 mg/kg BW) in the LPS injection groups, which would be sampled at 5 time points (1 h post-injection [**hpi**], 2 hpi, 4 hpi, 6 hpi, and 8 hpi). Results showed that tumor necrosis factor-α mRNA transcription in duodenal tissue increased gradually since 1 hpi, peaked at 4 hpi, and then reduced remarkably, indicating that 4 hpi of LPS was the early stage of intestinal inflammation. Meanwhile, the *MUC2* expression in duodenal tissue was dramatically reduced since 1 hpi of LPS. The ISC marker, *Lgr5* and *Bmi1*, in the duodenal crypt were reduced from 1 hpi to 4 hpi and elevated later. Accordingly, the hydroethidine staining showed that the reactive oxygen species level, which drives the differentiation of ISC, in the duodenal crypt reduced obviously at 1 hpi and recovered gradually since 4 hpi. The analysis of Paneth cells showed that many swollen mitochondria appeared in Paneth cells at 4 hpi of LPS. Meanwhile, the *Lysozyme* transcription in the duodenal crypt was substantially decreased since 1 hpi of LPS. However, the *Wnt3a* and *Dll1* in duodenal crypt decreased at 1 hpi of LPS, then increased gradually. In conclusion, Paneth cells were impaired at the early stage of intestinal inflammation, then recovered rapidly. Thus, the ISC activity was reduced at first and recovery soon.

Key words: Paneth cell, intestinal stem cell, goblet cell, inflammation, chicken

2021 Poultry Science 100:615–622
https://doi.org/10.1016/j.psj.2020.11.055

INTRODUCTION

Dozens of complex factors will induce intestinal inflammation, which challenges the integrity of the intestinal mucosa. Apart from histomorphologic changes, intestinal inflammation could also lead to dramatic changes in inflammatory cytokine. Tumor necrosis factor-α (**TNF-α**) is a major proinflammatory cytokine involved in the innate immunologic response induced by lipopolysaccharide (**LPS**) (Li et al., 2016). Tumor necrosis factor-α is one of the most abundant early mediators in inflamed tissue and rapidly released by macrophages after trauma, infection, or exposure to bacteria-derived LPS (Parameswaran and Patial, 2010). In the "cytokine release syndrome" BALB/c mice model, serum TNF-α level was maximal 30 min after anti-CD3 antibodies intraperitoneal injection and declined gradually after that (Radojevic et al., 1999). Hence, TNF-α was used as an early indicator of intestinal inflammation in the present study.

The intestinal mucosa consists of enterocytes, goblet cells, Paneth cells, enteroendocrine cells, and intestinal stem cells, and so on. Among them, goblet cells play a critical role in producing and preserving a protective mucus blanket on intestinal mucosa through synthesizing and secreting high-molecular-weight glycoproteins known as mucins (Kim and Khan, 2013). Infection or inflammation could influence the amount and secretory function of the goblet cells. Zhu et al. (2020) demonstrated that, in young chickens, *Salmonella* Pullorum infection could induce a significant loss of goblet cells and noticeable reduced *MUC2* expression. However, in the chicken, the change of goblet cells at the early stage of intestinal inflammation is unclear.

Received October 16, 2020.
Accepted November 23, 2020.

[1]These authors contributed equally to this work.

[2]Corresponding author: lijiannp@zju.edu.cn

Intestinal stem cells (**ISC**) are located at the crypt bottom and can differentiate into various epithelia (Sato et al., 2011). Generally, ISC including rapidly cycling ISC, which are markered by Lgr5, Olfm4, and Znrf3 (Barker et al., 2007, 2012; van der Flier et al., 2009), and slowly cycling reserve ISC, which are mainly located at "+4" stem cell zone and markered by Bmi1 and Hopx (Takeda et al., 2011). The activity and development of ISC can be influenced by infection or inflammation. Studies have shown that acute intestinal inflammation in mice was accompanied with a dramatic loss of ISC (Richmond et al., 2018; Schmitt et al., 2018), whereas the evoked interferon gamma and TNF-α would activate the regeneration of reserve ISC (Richmond et al., 2018). Moreover, Helminth infection in mice could promote intestinal mucosal tuft cells to secrete IL-25, which further promote group 2 innate lymphoid cells to secret IL-13, and finally induce ISC to differentiate into tuft cells and goblet cells (Howitt et al., 2016; von Moltke et al., 2016). However, in chickens, how the fate of ISC changes at the early stage of intestinal inflammation is unclear and is the basis for investigating mucosal repair after injury.

Paneth cells are an essential component in the crypt, which served as the niche for ISC development. As a niche component, Paneth cells could secret Wnt3 and Notch ligand Delta-like1 (**Dll1**) and Delta-like4, which further acted on adjacent ISC (van Es et al., 2012; Farin et al., 2016). Nevertheless, the fate and secretory function of Paneth cells are changing during infection and inflammation. In mice, *Salmonella* infection could increase Paneth cells' amount (Haber et al., 2017). In humans, a high level of TNF-α, which presented in the lamina propria of the inflamed ileum, was demonstrated to induce the necroptosis of Paneth cells (Günther et al., 2011). In rats, interferon gamma evoked by *Toxoplasma gondii* infection could activate autophagy in Paneth cells and further promote mucosal renewal (Burger et al., 2018). However, in chickens, how the function of Paneth cells changes at the early stage of intestinal inflammation and further influences ISC development is unclear and is the key to understand the mechanism of mucosal repair after injury.

In the present study, we sought to investigate the alteration of the chicken's Paneth cells and further uncover the mechanism that ISC activity altered at the early stage of intestinal inflammation.

MATERIALS AND METHODS

Experiment Design

A total of 36 HyLine White chickens (*Gallus*) at the age of 7 d were randomly divided into 6 groups (1 control group and 5 LPS injection groups, n = 6). The chickens in the control group were injected (i.p.) with PBS (pH 7.4). The chickens in the LPS injection groups, which would be sampled at 5 time points (1 h postinjection [**hpi**], 2 hpi, 4 hpi, 6 hpi, and 8 hpi), were injected (i.p.) with LPS (10 mg/kg BW, L2880; Sigma, St. Louis, MO). After that, the duodenal tissue and duodenal crypt were sampled from 6 individuals in each group, then stored in liquid nitrogen, 4% paraformaldehyde, or 2.5% glutaraldehyde until analyzing. The present study was carried out following the Guiding Principles for the Care and Use of Laboratory Animals of Zhejiang University. The experimental protocols were approved by the Committee on the Ethics of Animal Experiments of Zhejiang University.

Duodenal Crypt Isolation

For investigating the niche for ISC, the duodenal crypt was isolated. As per the previous protocol (Li et al., 2018), the duodenum was removed and washed in PBS after longitudinally cutting. Then, they were cut into 1- to 2-cm segments and shaken gently in 2 mmol cold EDTA (pH 7.4) for 30 min thrice. After that, the suspension was passed through a 70-μm nylon cell strainer (352360; Corning, NY) and was further purified by centrifuging (100 × *g*) and resuspending. The collected crypts were used for further analysis.

Histologic Study

The duodenal samples fixed in 4% paraformaldehyde were embedded by paraffin, then the cross sections (5 μm) were prepared for morphologic study. The phloxine-tartrazine staining was performed to identify Paneth cells by their characteristic purple granules. Briefly, the paraffin cross sections were stained by hematoxylin, then dipped in solution A, a mixture of 0.5 g phloxine B (18,472-87-2; Aladdin, Shanghai, China) and 0.5 g calcium chloride dissolved in 100 mL distilled water, for 20 min. After rinsing in tap water, the cross sections were placed in solution B, a saturated solution formed by tartrazine (1934-21-0; Aladdin, Shanghai, China) dissolved in 100 mL 2-ethoxy ethanol, until characteristic purple granules appeared and all other tissue was yellow.

Transmission Electron Microscopy

The duodenal samples prepared for transmission electron microscopy (**TEM**) assay were fixed with 2.5% glutaraldehyde (at 4°C overnight) and 1% osmium acid (at room temperature for 2 h). Each fixation was followed by 15 min rinse with 0.1 M PBS (pH 7.0) three times. After fixation, the samples were dehydrated with a graded ethanol series (30, 50, 70, 80, 90, and 95% for 15 min each, 100% for 20 min). First, samples were infiltrated in a mixture of Spurr and acetone (vol/vol = 1:1 for 1 h, vol/vol = 3:1 for 3 h) and then in Spurr overnight. The following day, the samples were embedded in Spurr and baked at 70°C overnight. Ultrathin sections (70–90 nm) were made by a Leica UC 7 ultramicrotome and then stained with lead citrate and saturated uranyl acetate in 50% ethanol for 5 to 10 min each. Finally, the ultrastructure of the crypt was observed by a Hitachi H-7650 TEM.

Hydroethidine Staining

For detecting the reactive oxygen species (**ROS**) level in the crypt, hydroethidine staining was performed. Hydroethidine is a superoxide indicator, where it intercalates within the cell's DNA, staining its nucleus a bright fluorescent red. As per the product manual, the frozen sections were rinsed with PBS three times, then incubated with 15 μmol hydroethidine (D23107; ThermoFisher Scientific, Waltham, MA) in dark at 37°C for 20 min. The nuclei were then counterstained with DAPI (300 nmol, MBD0020; Sigma, St. Louis, MO). Finally, the sections were mounted with the antifade solution (C1210; Applygen Technologies Inc., Beijing, China).

Quantitative Real-Time PCR

Total RNA from the duodenal tissue and duodenal crypt were extracted using TRIzol reagent and reverse transcribed into cDNA using the SuperScript First-Strand Synthesis System (11904018; ThermoFisher Scientific, Waltham, MA). The cDNA was used as a template for quantitative real-time PCR (**qPCR**) in a reaction system: 1.5 μL cDNA, 400 nM primers, 7.5 μL 2 × SYBR qPCR Master Mix (Q711-02; Vazyme Biotech Co., Ltd., Nanjing, China). The qPCR reactions were performed in a CFX96 Touch real-time PCR system with cycling conditions as follows: 95°C for 30 s, 40 cycles of 95°C 10 s followed by 60°C 30 s. The sequences of primers were listed as follows: *TNF-α* (192 bp, NM_204267.1, Forward: ACCCGTAGTGC TGTTCTATGACC; Reverse: TGTTCCACATCTTT-CAGAGCATC); *MUC2* (161 bp, NM_001318434.1, Forward: TACTTCACCTTCAACCATTACAAC; Reverse: CATAGTCACCACCATCTTCTTCA); *Lgr5* (115 bp, XM_425441.4, Forward: CTTCTCTTCGTT CTCTGGATTTAGC; Reverse: GAGGACAAAAGGT TGGATGAC); *Bmi1* (104 bp, NM_001007988.1, Forward: AGTTCCTGCGGAGTAAGATGG; Reverse: GTAGGCAATGTCCATCAGCGT); *Lysozyme* (142 bp, NM_205281.1, Forward: TCTTTGGAC-GATGTGAGCTG; Reverse: CCATCGGTGTTACGG TTTGT); *Dll1* (127 bp, NM_204973.2, Forward: TGA ACTACTGCACTCACCACAA; Reverse: TCGTTG ATTTCAATCTCGCAGC); *Wnt3a* (200 bp, NM_001 171601.1, Forward: CTTCTTCAAGGCTCCGACTG; Reverse: GGCACTTCTCTTTCCGTTTC); *GAPDH* (116 bp, NM_204305, Forward: GATGGGTGTCAAC-CATGAGAAA; Reverse: CAATGCCAAAGTTGT-CATGGA). All samples were repeated in triplicate, and all experiments were repeated more than three times. All samples were normalized with *GAPDH* using the comparative cycle threshold method ($2^{-[\triangle][\triangle]Ct}$).

Statistical Analysis

Statistical analysis was performed using SPSS 16.0. The statistical significance among various groups was examined by one-way ANOVA followed by the least significant difference. The significance level was set at P-value < 0.05.

RESULTS

The Response of Duodenal Tissue to LPS-Induced Intestinal Inflammation

For identifying the early stage of intestinal inflammation, the 7-day-old chickens were injected with LPS and the mRNA transcription of duodenal *TNF-α*, which is an early indicator of inflammation, at various time points after LPS treatment was analyzed. As shown in Figure 1A, compared with the control group, the duodenal *TNF-a* level in the LPS group increased gradually since 1 hpi of LPS, peaked at 4 hpi of LPS (higher than the control group by 191.52%, P-value < 0.0001) and then reduced dramatically. These indicate that 4 hpi of LPS was the early stage of intestinal inflammation. Furthermore, after LPS treatment, the *MUC2* mRNA transcription (Figure 1B) was reduced gradually from 1 hpi to 8 hpi and presented statistical significance with the control group after 2 hpi (lower by 58.27–94.79%, P-value < 0.001).

The Response of ISC to LPS-Induced Intestinal Inflammation

As ROS drives differentiation of ISC, hydroethidine staining was performed to assay the ROS level in the crypt. As shown in Figure 2A, in the control group, the nucleus in the crypt showed bright fluorescent red, especially at the crypt bottom. However, after LPS injection, the fluorescence intensity weakened obviously at 1 hpi, then recovered gradually from 4 hpi to 8 hpi.

For analyzing the alteration of ISC activity after LPS treatment, the relative expression of *Lgr5* (ISC marker) and *Bmi1* (quiescent +4 position ISC marker) in the duodenal crypt was analyzed. The qPCR results (Figures 2B and 2C) showed that after LPS treatment, *Lgr5* and *Bmi1* were decreased gradually from 1 hpi to 4 hpi, then elevated at 8 hpi. At 4 hpi of LPS, *Lgr5* and *Bmi1* were lower by 53.78% (P-value = 0.040) and 34.78% (P-value = 0.119) than the control group, respectively. However, at 8 hpi of LPS, *Lgr5* and *Bmi1* were elevated and comparable with the control group.

Morphologic Alteration of Paneth Cells Induced by LPS Injection

For identifying the morphologic alteration of Paneth cells at the early stage of intestinal inflammation, the phloxine-tartrazine staining and TEM assay was performed. Under phloxine-tartrazine staining, the characteristic purple granules of Paneth cells were presented at the crypt bottom of both control and LPS-4 hpi groups (Figures 3A–3D, red arrowhead). Under TEM assay, Paneth cells were identified by their

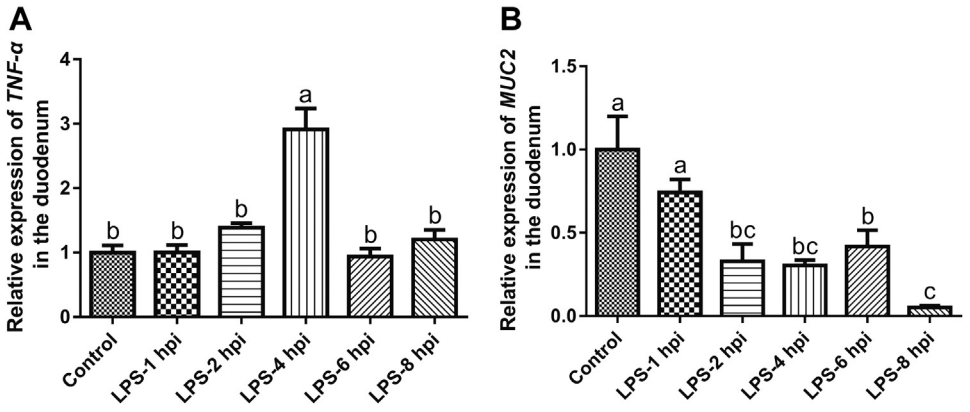

Figure 1. The response of duodenal tissue to lipopolysaccharide (LPS)-induced intestinal inflammation. Histograms represented the analysis of *TNF-α* mRNA transcription (A) and *MUC2* mRNA transcription (B) in the duodenal tissue from the control group and LPS injection groups (sampled at 1 h post-injection [hpi], 2 hpi, 4 hpi, 6 hpi and 8 hpi). Values with no common letters are significantly different ($P < 0.05$).

elongated, flattened nucleus, large cytoplasm, and secretory granules (Figure 3E, white star). Meanwhile, ISC were identified by their wedge-shaped nuclei (Figure 3E, white triangle), which were located between Paneth cells. At 4 hpi of LPS, when compared with the mitochondria in the control group (Figure 3F, white arrow), a considerable number of mitochondria in Paneth cells were swollen (Figures 3E and 3G, white arrow).

Secretory Functional Alteration of Paneth Cells Induced by LPS Injection

The Lysozyme (Paneth cell marker), Wnt3a (regulate Lgr5 gene), and Dll1 (key Notch ligand) were mainly secreted by Paneth cells, which further constitute the metabolic niche for nearby ISC. In the present study, mRNA expression of *Lysozyme*, *Wnt3a*, and *Dll1* in the duodenal crypt was analyzed by qPCR. The results

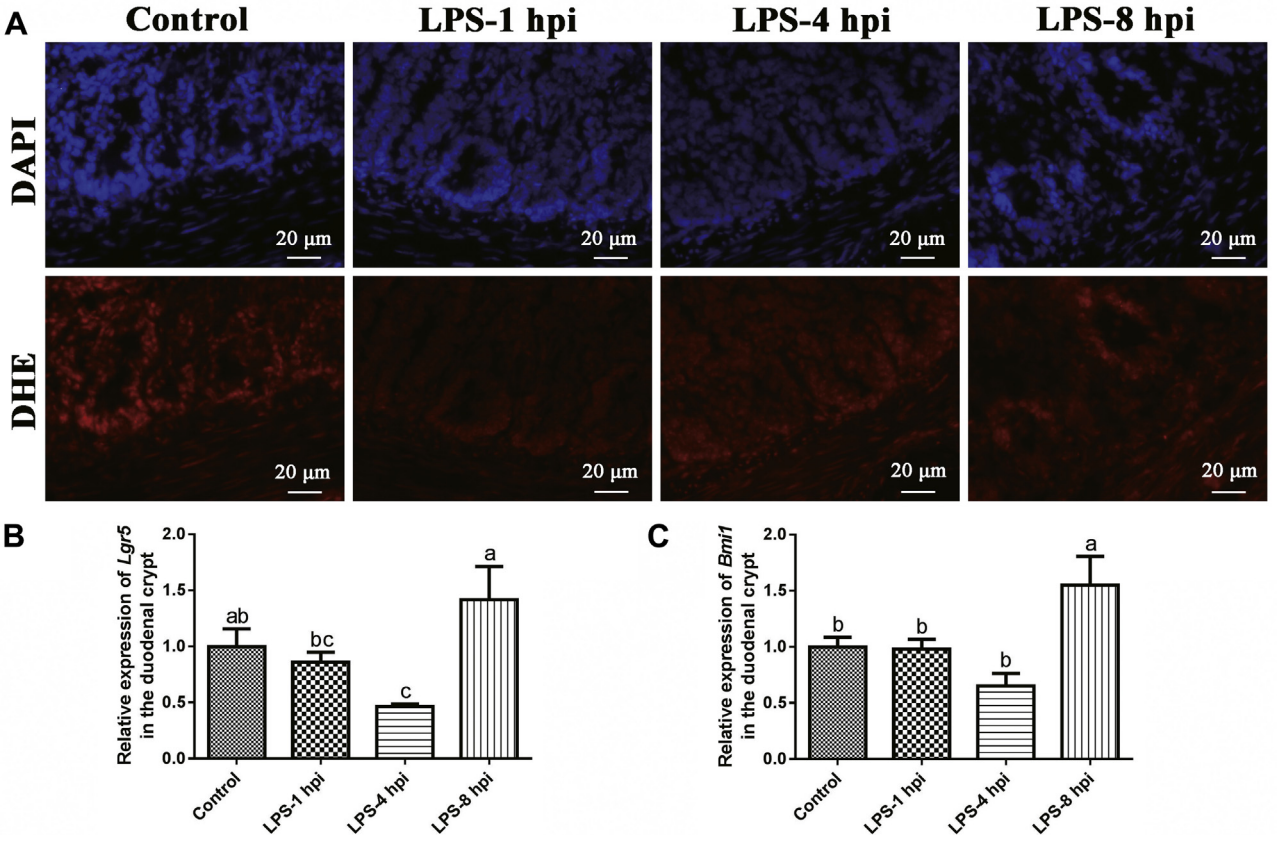

Figure 2. Alteration of intestinal stem cells (ISC) activity induced by lipopolysaccharide (LPS) injection. (A) The hydroethidine (DHE) staining showed the reactive oxygen species in the duodenal crypt, DAPI counterstained the nuclei, scale bar = 20 μm. Histograms represented the relative expression of ISC marker *Lgr5* mRNA (B) and *Bmi1* mRNA (C) in the duodenal crypt from the control group and LPS injection groups (sampled at 1 h post-injection [hpi], 4 hpi, and 8 hpi). Values with no common letters are significantly different ($P < 0.05$).

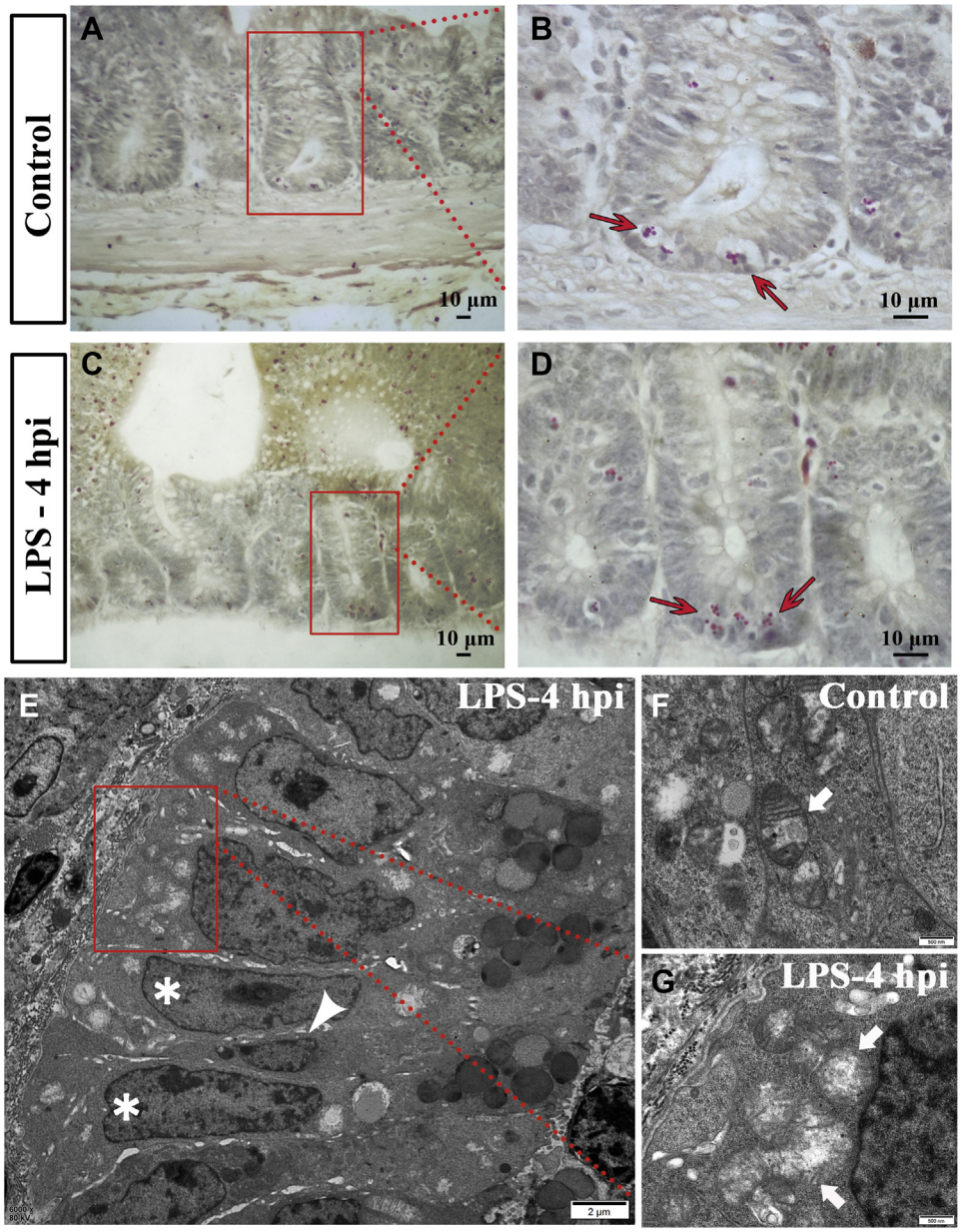

Figure 3. Morphologic alteration of Paneth cells induced by lipopolysaccharide (LPS) injection. (A–D) On phloxine-tartrazine staining, the characteristic purple granular of Paneth cells were presented at the crypt bottom (red arrowhead), scale bar = 10 μm. (E) On transmission electron microscopy assay, Paneth cells (white star) were identified by their elongated, flattened nucleus, large cytoplasm, and secretory granules. Intestinal stem cells (white triangle) were identified by their wedge-shaped nuclei, located between Paneth cells, scale bar = 2 μm. Compared with the mitochondria in the control group (F, white arrow), many mitochondria in the LPS-4 hpi group were swollen (G, white arrow), scale bar = 500 nm. Abbreviation: hpi, h postinjection.

(Figure 4) showed that the *Lysozyme* expression on LPS injection was considerably lower than that in the control group (by 72.56–90.78%, *P*-value < 0.0001). However, *Wnt3a* and *Dll1* decreased at 1 hpi of LPS, then increased gradually. At 8 hpi of LPS, *Wnt3a* and *Dll1* in the crypt were higher by 36.88% (*P*-value = 0.168) and 96.46% (*P*-value = 0.001), respectively, than those in the control group.

DISCUSSION

The amount and secretory function of the goblet cells could be affected by infection or inflammation. In young chickens that were infected with *S.* Pullorum, a significantly reduced *MUC2* expression was observed in the chicken intestine (Zhu et al., 2020). In the present study, with the progress of intestinal inflammation induced by LPS, the *MUC2* transcription level decreased rapidly since 1 hpi. Owing to the upregulated *Dll1* in the crypt at 8 hpi of LPS, which would repress the differentiation of ISC into the secretory lineage, the *MUC2* transcription level declined at 8 hpi of LPS. Birchenough et al. (2015) pointed out that in an inflammatory or infectious condition, the intestinal goblet cell proliferation and mucous secretion are under direct regulation by the immune system. We speculated that in young chickens, the

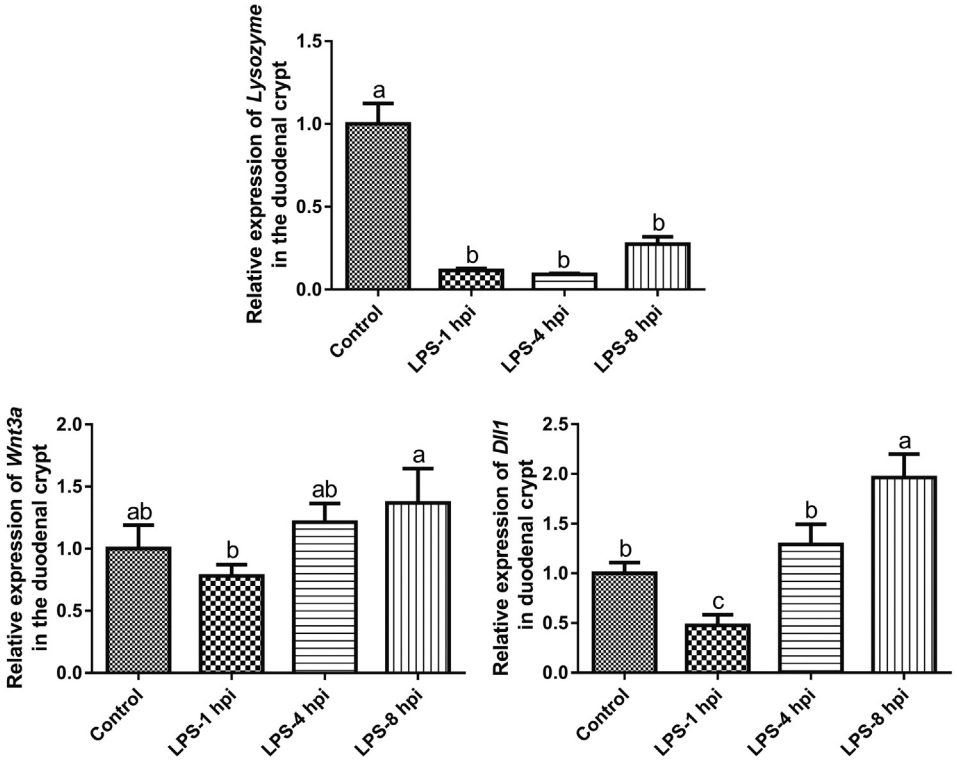

Figure 4. Secretory alteration of Paneth cells induced by lipopolysaccharide (LPS) injection. Histograms represented the relative expression of *Lysozyme*, *Wnt3a* and *Dll1* mRNA in the duodenal crypt from control group and LPS injection groups (sampled at 1 h postinjection [hpi], 4 hpi, and 8 hpi). Values with no common letters are significantly different ($P < 0.05$).

reduction of *MUC2* at the early stage is a direct reaction of mucosa to inflammation. However, the decrease of *MUC2* later could be induced by the alteration of ISC niche.

Lgr5$^+$ ISC can differentiate into various epithelia and maintain epithelial self-renew. Previously, IL-22, IL-25, and IL-13 were proved to regulate Lgr5$^+$ ISC regeneration or differentiation (Lindemans et al., 2015; Howitt et al., 2016; von Moltke et al., 2016). Besides, nutritional state and inflammation have been identified as upstream regulators of ISC activity in mammal (Beumer and Clevers, 2016). In the present study, after LPS treatment, *Lgr5* and *Bmi1* in the duodenal crypt were decreased gradually from 1 hpi to 4 hpi, then elevated at 8 hpi. Similarly, in S. Pullorum–infected chickens, the expression of ISC markers *Lgr5* and *Bmi1* was increased to support the crypt hyperplasia (Xie et al., 2020). As the ROS signaling in ISC was proved to activate p38 and drive the differentiation of ISC (Rodríguez-Colman et al., 2017). Our study further confirmed that the ROS level in the duodenal crypt decreased obviously at 1 hpi of LPS and then recovered gradually. Taken together, we suggested that the LPS-induced intestinal inflammation would reduce the ISC activity at an early stage (such as from 1 hpi to 4 hpi) and recover soon (such as at 8 hpi).

Paneth cells are a primary secretory epithelium that resides at the crypt bottom and releases antimicrobial peptides, including lysozyme. Our study demonstrated that after LPS injection, *Lysozyme* expression in duodenal crypt decreased substantially from 1 hpi to 8 hpi. This result aligns well with the finding that *Salmonella enterica* serovar Typhimurium infected in mice would reduce the Paneth cell–specific lysozyme content and the number of granules per Paneth cell (Martinez Rodriguez et al., 2012). However, the Paneth cell population would expand owing to the activation of their differentiation program (Martinez Rodriguez et al., 2012). Moreover, ultrastructural analysis in our study showed a considerable number of mitochondria in Paneth cells were swollen at 4 hpi of LPS, indicating that the Paneth cells impaired severely under LPS challenge. Similarly, necrosis-like swelling mitochondria also appeared in the intestinal crypt of mice with inflammatory bowel disease (Wang et al., 2020). These suggested that Paneth cells of chickens impaired obviously at the early stage of intestinal inflammation.

Paneth cells provide a niche for ISC by producing signaling molecules such as Wnt, Notch ligands, and epidermal growth factor (Schepers et al., 2012). Rodríguez-Colman et al. (2017) proved that Wnt3a would promote the proliferation of Lgr5$^+$ ISC and transit-amplifying cells in intestinal organoid in vitro. van Es et al. (2012) suggested that Paneth cells could secret Dll1 and Delta-like4 as Notch ligands, which trigger Notch1 and Notch2 on ISC, thus keeping them from entry into the secretory lineage. In the present study, after LPS challenge in young chickens, *Dll1* and *Wnt3a* in the crypt increased gradually from 1 hpi to 8 hpi, corresponding to the downregulated *MUC2* expression and upregulated *Lgr5* and *Bmi1* at 8 hpi. Consistently, TNF was demonstrated to enhance Wnt/β-catenin

signaling during ulcer healing in mice with inflammatory bowel disease (Bradford et al., 2017). *S.* Pullorum infection in chickens could increase the depth of crypt and abnormal proliferation of ISC by overactivation of Wnt/β-catenin pathway (Xie et al., 2020). These suggested that the secretion profile of the chicken's Paneth cells was changed under LPS-induced intestinal inflammation.

In conclusion, at the early stage of LPS-induced intestinal inflammation (from 1 hpi–4 hpi), Paneth cells were impaired obviously, which was reflected as swollen mitochondria and downregulated *Lysozyme*. Subsequently, the ISC activity reduced remarkably. Soon after that, the transcription of *Wnt3a* and *Dll1* in crypt increased gradually and induced the recovery of ISC activity.

ACKNOWLEDGMENTS

This study was supported by the National Natural Science Foundation of China (No. 31972630) and the Undergraduate Student Scientific Research Practice Program of Zhejiang University (No. P2020061). We are grateful to Weidong Zeng (Zhejiang University) and the Experimental Teaching Center (College of Animal Sciences, Zhejiang University) for help in the experiments.

DISCLOSURES

This manuscript represents original material that has not been published, is not being considered for publication elsewhere, and that all animals used in the research were treated humanely according to the Guiding Principles for the Care and Use of Laboratory Animals of Zhejiang University. The experimental protocols were approved by the Committee on the Ethics of Animal Experiments of Zhejiang University. All authors have read the manuscript and agree that the work is ready for submission to the journal and they accept the responsibility for the manuscript's content. The study is performed in accordance with guidelines of ***Poultry Science.***

REFERENCES

Barker, N., J. H. van Es, J. Kuipers, P. Kujala, M. van den Born, M. Cozijnsen, A. Haegebarth, J. Korving, H. Begthel, P. J. Peters, and H. Clevers. 2007. Identification of stem cells in small intestine and colon by marker gene *Lgr5*. Nature 449:1003–1007.

Barker, N., A. van Oudenaarden, and H. Clevers. 2012. Identifying the stem cell of the intestinal crypt: strategies and pitfalls. Cell Stem Cell 11:452–460.

Beumer, J., and H. Clevers. 2016. Regulation and plasticity of intestinal stem cells during homeostasis and regeneration. Development 143:3639–3649.

Birchenough, G. M. H., M. E. V. Johansson, J. K. Gustafsson, J. H. Bergström, and G. C. Hansson. 2015. New developments in goblet cell mucus secretion and function. Mucosal Immunol. 8:712–719.

Bradford, E. M., S. H. Ryu, A. P. Singh, G. Lee, T. Goretsky, P. Sinh, D. B. Williams, A. L. Cloud, E. Gounaris, V. Patel, O. F. Lamping, E. B. Lynch, M. P. Moyer, I. G. De Plaen, D. J. Shealy, G. Y. Yang, and T. A. Barrett. 2017. Epithelial TNF Receptor signaling promotes mucosal repair in inflammatory bowel disease. J. Immunol. 199:1886–1897.

Burger, E., A. Araujo, A. López-Yglesias, M. W. Rajala, L. Geng, B. Levine, L. V. Hooper, E. Burstein, and F. Yarovinsky. 2018. Loss of Paneth cell autophagy causes acute susceptibility to *Toxoplasma gondii*-mediated inflammation. Cell Host Microbe 23:177–190.e4.

Farin, H. F., I. Jordens, M. H. Mosa, O. Basak, J. Korving, D. V. F. Tauriello, K. de Punder, S. Angers, P. J. Peters, M. M. Maurice, and H. Clevers. 2016. Visualization of a short-range Wnt gradient in the intestinal stem-cell niche. Nature 530:340–343.

Günther, C., E. Martini, N. Wittkopf, K. Amann, B. Weigmann, H. Neumann, M. J. Waldner, S. M. Hedrick, S. Tenzer, M. F. Neurath, and C. Becker. 2011. Caspase-8 regulates TNF-α-induced epithelial necroptosis and terminal ileitis. Nature 477:335–339.

Haber, A. L., M. Biton, N. Rogel, R. H. Herbst, K. Shekhar, C. Smillie, G. Burgin, T. M. Delorey, M. R. Howitt, Y. Katz, I. Tirosh, S. Beyaz, D. Dionne, M. Zhang, R. Raychowdhury, W. S. Garrett, O. Rozenblatt-Rosen, H. N. Shi, O. Yilmaz, R. J. Xavier, and A. Regev. 2017. A single-cell survey of the small intestinal epithelium. Nature 551:333–339.

Howitt, M. R., S. Lavoie, M. Michaud, A. M. Blum, S. V. Tran, J. V. Weinstock, C. A. Gallini, K. Redding, R. F. Margolskee, L. C. Osborne, D. Artis, and W. S. Garrett. 2016. Tuft cells, taste-chemosensory cells, orchestrate parasite type 2 immunity in the gut. Science 351:1329–1333.

Kim, J. J., and W. I. Khan. 2013. Goblet cells and mucins: role in innate defense in enteric infections. Pathogens 2:55–70.

Li, J., J. Li, Jr, S. Y. Zhang, R. X. Li, X. Lin, Y. L. Mi, and C. Q. Zhang. 2018. Culture and characterization of chicken small intestinal crypts. Poult. Sci. 97:1536–1543.

Li, N., Y. B. Song, W. Zhao, T. T. Han, S. H. Lin, O. Ramirez, and L. Liang. 2016. Small interfering RNA targeting NF-κB attenuates lipopolysaccharide-inducedacute lung injury in rats. BMC Physiol. 16:7.

Lindemans, C. A., M. Calafiore, A. M. Mertelsmann, M. H. O'Connor, J. A. Dudakov, R. R. Jenq, E. Velardi, L. F. Young, O. M. Smith, G. Lawrence, J. A. Ivanov, Y. Y. Fu, S. Takashima, G. Hua, M. L. Martin, K. P. O'Rourke, Y. H. Lo, M. Mokry, M. Romera-Hernandez, T. Cupedo, L. Dow, E. E. Nieuwenhuis, N. F. Shroyer, C. Liu, R. Kolesnick, M. R. M. van den Brink, and A. M. Hanash. 2015. Interleukin-22 promotes intestinal-stem-cell-mediated epithelial regeneration. Nature 528:560–564.

Martinez Rodriguez, N. R., M. D. Eloi, A. Huynh, T. Dominguez, A. H. C. Lam, D. Carcamo-Molina, Z. Naser, R. Desharnais, N. H. Salzman, and E. Porter. 2012. Expansion of Paneth cell population in response to enteric *Salmonella enterica* serovar Typhimurium infection. Infect. Immun. 80:266–275.

Parameswaran, N., and S. Patial. 2010. Tumor necrosis factor-α signaling in macrophages. Crit. Rev. Eukaryot. Gene Expr. 20:87–103.

Radojevic, N., D. M. Mckay, M. Merger, B. A. Vallance, S. M. Collins, and K. Croitoru. 1999. Characterization of enteric functional changes evoked by in vivo anti-CD3 T cell activation. Am. J. Physiol. 276:715–723.

Richmond, C. A., H. Rickner, M. S. Shah, T. Ediger, L. Deary, F. Zhou, A. Tovaglieri, D. L. Carlone, and D. T. Breault. 2018. JAK/STAT-1 signaling is required for reserve intestinal stem cell activation during intestinal regeneration following acute inflammation. Stem Cell Rep. 10:17–26.

Rodríguez-Colman, M. J., M. Schewe, M. Meerlo, E. Stigter, J. Gerrits, M. Pras-Raves, A. Sacchetti, M. Hornsveld, K. C. Oost, H. J. Snippert, N. Verhoeven-Duif, R. Fodde, and B. M. T. Burgering. 2017. Interplay between metabolic identities in the intestinal crypt supports stem cell function. Nature 543:424–427.

Sato, T., J. H. van Es, H. J. Snippert, D. E. Stange, R. G. Vries, M. van den Born, N. Barker, N. F. Shroyer, M. van de Wetering, and H. Clevers. 2011. Paneth cells constitute the niche for Lgr5 stem cells in intestinal crypts. Nature 469:415–418.

Schepers, A. G., H. J. Snippert, D. E. Stange, M. van den Born, J. H. van Es, M. van de Wetering, and H. Clevers. 2012. Lineage tracing reveals $Lgr5^{+}$ stem cell activity in mouse intestinal adenomas. Science 337:730–735.

Schmitt, M., M. Schewe, A. Sacchetti, D. Feijtel, W. S. van de Geer, M. Teeuwssen, H. F. Sleddens, R. Joosten, M. E. van Royen,

H. J. G. van de Werken, J. van Es, H. Clevers, and R. Fodde. 2018. Paneth cells respond to inflammation and contribute to tissue regeneration by acquiring stem-like features through SCF/c-Kit signaling. Cell Rep 24:2312–2328.e7.

Takeda, N., R. Jain, M. R. LeBoeuf, Q. Wang, M. M. Lu, and J. A. Epstein. 2011. Interconversion between intestinal stem cell populations in distinct niches. Science 334:1420–1424.

van der Flier, L. G., A. Haegebarth, D. E. Stange, M. van de Wetering, and H. Clevers. 2009. OLFM4 is a robust marker for stem cells in human intestine and marks a subset of colorectal cancer cells. Gastroenterology 137:15–17.

van Es, J. H., T. Sato, M. van de Wetering, A. Lyubimova, A. N. Y. Nee, A. Gregorieff, N. Sasaki, L. Zeinstra, M. van den Born, J. Korving, A. C. M. Martens, N. Barker, A. van Oudenaarden, and H. Clevers. 2012. Dll1^{+} secretory progenitor cells revert to stem cells upon crypt damage. Nat. Cell Biol. 14:1099–1104.

von Moltke, J., M. Ji, H. E. Liang, and R. M. Locksley. 2016. Tuft-cell-derived IL-25 regulates an intestinal ILC2-epithelial response circuit. Nature 529:221–225.

Wang, R. C., H. D. Li, J. F. Wu, Z. Y. Cai, B. Z. Li, H. X. Ni, X. F. Qiu, H. Chen, W. Liu, Z. H. Yang, M. Liu, J. Hu, Y. J. Liang, P. Lan, J. H. Han, and W. Mo. 2020. Gut stem cell necroptosis by genome instability triggers bowel inflammation. Nature 580:386–390.

Xie, S., Y. C. Li, S. Y. Zhao, Y. J. Lv, and Q. H. Yu. 2020. *Salmonella* infection induced intestinal crypt hyperplasia through Wnt/β-catenin pathway in chicken. Res. Vet. Sci. 130:179–183.

Zhu, L. D., X. X. Lu, L. Liu, J. Voglmeir, X. Zhong, and Q. H. Yu. 2020. *Akkermansia muciniphila* protects intestinal mucosa from damage caused by *S.* pullorum by initiating proliferation of intestinal epithelium. Vet. Res. 51:34.